

## Application of Rank Annihilation Factor Analysis to the Determination of the Stability Constant of the Complex XL and Rate Constants for the Reaction of X and XL with the Reagent Z Using Kinetic Profiles

Abbas Afkhami\* and Lida Khalafi

Faculty of Chemistry, Bu-Ali-Sina University, Hamadan 65174, Iran

Received November 21, 2006; E-mail: Afkhami@basu.ac.ir

A simple procedure for the kinetic spectrophotometric determination of the formation constant of 1:1 (XL) complexes (or adducts) using rank annihilation factor analysis (RAFA) is proposed. The method was based on the effect of the concentration of L (or X) on the reaction of X (or L) with a reagent (Z). The rate constants for the reactions of X (or L) and XL with Z were also determined. In order to perform RAFA, concentration profiles were calculated by optimizing the value of formation constant. The rank of the original data matrix was reduced by one by annihilating the information of X (or L). The best estimation of rate constant of complex XL reduced the rank of the system to zero (noise level). The performance of the method was evaluated using synthetic data as well as experimental data, and good results were obtained. The spectrophotometric data for the study of the effect of  $\beta$ -cyclodextrin ( $\beta$ -CD) on the oxidation reaction of some catechol derivatives with iodate at pH 3.60 was used as an example. The difference in the rate of the oxidation reaction of catechol derivatives with iodate at pH 3.60 in the presence of different concentrations of  $\beta$ -CD was monitored.

Kinetic profiles measured from a chemical reaction can form a two-way data matrix, which contains the reaction kinetic information and concentration of each component. Kinetic information, such as the reaction model and rate constants, can be obtained through analysis of the two-way spectroscopic data by means of proper chemometric algorithms. When the individual components in the reaction mixture have a dominating response spectral range, some common methods, such as non-linear least-squares fit, can be used to extract the kinetic information according to the absorbance data for a single wavelength.<sup>1,2</sup> Frequently, there are extensive kinetic and spectral overlap between components. Methods have been developed to resolve such two-way spectroscopic data across the entire spectral range. Bijlsma et al.<sup>3,4</sup> have made the two-way kinetic-spectral data into three-way data with time shifting and have proposed a method for determining the rate constants for a first-order reaction using a trilinear model. Furusjo and Danielsson<sup>5</sup> have proposed an approach based on refinement of concentration profiles from the kinetic model by target testing and have obtained the rate constants for first-order and second-order reactions.

Rank annihilation factor analysis (RAFA)<sup>6</sup> is an efficient chemometric technique, based on rank analysis for two-way data. It can be employed to analyze an unknown system quantitatively. RAFA, originally developed by Ho et al.<sup>7</sup> as an iterative procedure, has been modified by Lorber,<sup>8,9</sup> who has proposed a direct solution of standard eigenvalue problem. Sanchez and Kowalski<sup>10</sup> have extended the method to general cases in which some components may or may not exist and have obtained results by using a generalized rank annihilation method (GRAM). RAFA has also been used to analyze the two-way chromatographic spectral data<sup>11</sup> for the determination

of environmental pollutants, such as polycyclic aromatic compounds,<sup>12,13</sup> and the correction of several types of instrumental inconsistencies.<sup>14</sup> It has also been used to the spectrophotometric study of complex formation equilibria.<sup>15</sup>

Recently, we have reported the application of RAFA in the determination of the conditional acidity constant as a function of  $\beta$ -CD concentration for some organic acids.<sup>16</sup>

RAFA has also been applied to the analysis of kinetic profiles. Zhu et al. have applied it to a two-step first-order consecutive reaction, have used RAFA to resolve the two-way kinetic-spectral data from spectroscopic reactions, and have acquire rate constants and the absorption spectrum of each component.<sup>17</sup> Zhu, Xia, and Li have also used RAFA in the simultaneous determination of reaction order and rate constant from kinetic spectral data.<sup>18</sup>

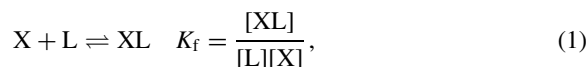
Cyclodextrins (CDs) are known to complex with a wide variety of molecules in their hydrophobic interior.<sup>19,20</sup> It has been determined that the binding forces involved in inclusion complexation are hydrophobic interactions, hydrogen binding, van der Waals forces, the release of high energy water from the CD cavity, and the relief of conformational strain upon guest inclusion.<sup>19–21</sup> It is important to study these weak interactions, to understand further how supramolecules form and to develop new approaches in pharmacy, analysis, and material science.<sup>21,22</sup> Imonigie and Macartney have reported the effects of  $\alpha$ - and  $\beta$ -CD inclusion of 4-*tert*-butylcatechol on the kinetics of its outer-sphere oxidation by transition-metal complexes in acidic aqueous media.<sup>23</sup> They have determined the magnitude of the inclusion stability of the complexes by <sup>1</sup>H and <sup>13</sup>C NMR spectroscopy.

In this work, we studied the application of RAFA to the determination of the stability constant of complex XL and

the rate constants for the reactions of X and XL with the reagent Z using kinetic profiles. To the best of our knowledge, in all of the reported works on the application of RAFA in spectrophotometric methods, the whole spectra have been used as a two-way matrix data (for example, see Refs. 16–18). In order to obtain the whole spectra with time in kinetic studies a diode array spectrophotometer is necessary that may not be available in each laboratory. However, in this work, we obtained two-way data by determining absorbance at a single wavelength by changing the concentration of reactant, and to our knowledge, this is the first report on the creation of a two-way matrix data by determining the absorbance at a single wavelength that can be obtained by a simple spectrophotometer, which is available in most laboratories. The method was applied to the determination of the formation constant for inclusion complexes of 4-*tert*-butylcatechol and 3-methylcatechol with  $\beta$ -CD and rate constant of their oxidation reaction with iodate as a typical example, by monitoring the effect of  $\beta$ -CD concentration on the oxidation reaction rate.

### Theoretical Background

By assuming the formation of a 1:1 complex between X and L, the complexation equilibrium can be written as:



where  $K_f$ ,  $[X]$ ,  $[L]$ , and  $[XL]$  stand for the formation constant of the complex XL and equilibrium concentrations of X, L, and XL, respectively.

By considering:

$$C_X = [XL] + [X], \quad (2)$$

and

$$[L] = C_L - [XL], \quad (3)$$

where  $C_X$  and  $C_L$  are analytical concentrations of X and L, respectively, it can be written:

$$[XL] = C_X - [X], \quad (4)$$

and

$$[L] = C_L - C_X + [X], \quad (5)$$

by substituting of Eqs. 4 and 5 into Eq. 1:

$$K_f = (C_X - [X]) / (C_L - C_X + [X])[X]. \quad (6)$$

By rearrangement of Eq. 6:

$$K_f[X]^2 + (K_f C_L - K_f C_X + 1)[X] - C_X = 0, \quad (7)$$

$[X] =$

$$\frac{-(K_f C_L - K_f C_X + 1) + ((K_f C_L - K_f C_X + 1)^2 - 4K_f C_X)^{0.5}}{2K_f}. \quad (8)$$

If both X and XL participate in the reaction with Z, and the rate constants for XL and X are different, at a pseudo-first-order reaction conditions, i.e. a large excess of Z and constant pH, it can be written:



$$C_{X,t} = C_{X,0} e^{-k't}, \quad (10)$$

$$C_{Q,t} = C_{X,0} - C_{X,t} = C_{X,0}(1 - e^{-k't}), \quad (11)$$

$$A_Q = \varepsilon_Q C_{X,0}(1 - e^{-k't}), \quad (12)$$

where Q stands for oxidation form of X,  $C_{X,0}$  is the initial concentration of X,  $C_{X,t}$  and  $C_{Q,t}$  are the concentrations of X and Q at time  $t$ , respectively,  $A$  is the absorbance at time  $t$ ,  $\varepsilon_Q$  is the molar absorptivities for Q, and  $k'$  is the pseudo-first-order rate constant for the above reaction. For the oxidation of XL with Z:



$$C_{XL,t} = C_{XL,0} e^{-k''t}, \quad (14)$$

$$C_{Q',t} = C_{XL,0} - C_{XL,t} = C_{XL,0}(1 - e^{-k''t}), \quad (15)$$

where  $Q'$  stands for oxidation form of XL,  $C_{XL,0}$  is the initial concentration of XL,  $C_{XL,t}$  and  $C_{Q',t}$  are the concentrations of XL and  $Q'$  at time  $t$ , respectively, and  $k''$  is the observed pseudo-first-order rate constant for the above reaction.  $k''$  is different from  $k'$ . Therefore, for overall reaction it can be written:

$$C_{Q_{tot},t} = C_{Q,t} + C_{Q',t} \\ = C_{X,0}(1 - e^{-k't}) + C_{XL,0}(1 - e^{-k''t}). \quad (16)$$

If the absorbance is monitored at  $\lambda_{max}$  for one of the products and if the absorption spectra for the products Q and  $Q'$  overlap, where the molar absorptivity for the other species in the solution at this wavelength is zero, then:

$$A = A_Q + A_{Q'}, \quad (17)$$

$$A = \varepsilon_Q C_{X,0}(1 - e^{-k't}) + \varepsilon_{Q'} C_{XL,0}(1 - e^{-k''t}), \quad (18)$$

where  $A$  is the total absorbance at time  $t$ , and  $A_Q$  and  $A_{Q'}$  are absorbance of Q and  $Q'$  at time  $t$ , respectively.  $\varepsilon_Q$  and  $\varepsilon_{Q'}$  are the molar absorptivities for Q and  $Q'$ , respectively.

As the amount of the complex formed depends on the concentration of L and the rate constants for XL and X are different, then the reaction rate depends on the concentration of L. Therefore, different kinetic profiles can be obtained for different concentrations of L. The kinetic profile can then be considered as a two-way matrix.

The concentration profile of X and XL can be calculated from Eq. 8 by substituting of proper  $K_f$  values. The concentrations of X and XL at various concentrations of L can form two column vectors  $C_{X,0}$  and  $C_{XL,0}$ . A two-way data matrix  $A$  with rank 2 can be formed from each kinetic profile.

$$A = A_Q + A_{Q'} + E \\ = C_{X,0} y_X^T + C_{XL,0} y_{XL}^T + E = CY^T + E, \quad (19)$$

where  $A_Q$  and  $A_{Q'}$  are the bilinear measuring matrix of pure X and XL and can be decomposed into the corresponding concentration profiles  $C_{X,0}$  and  $C_{XL,0}$  (column vectors) and the kinetic profiles  $y_X^T$  and  $y_{XL}^T$  (row vector, superscript T denotes the transpose of a matrix or vector).  $C$  and  $Y^T$  represent matrices formed, by the concentration and the kinetic profiles of each species, respectively.  $E$  is the residual matrix and should contain only noise. As mentioned above for different kinetic profiles the concentrations of L are different and all other parameters are constant. The kinetic profiles were obtained under pseudo-first-order reaction conditions.

The size of matrix  $A$  is  $c \times t$ , where  $c$  denotes the number of  $L$  concentrations and  $t$  is the number of times in which the absorbances were recorded ( $c$  is smaller than  $t$ ). Obviously, the size of matrices  $C$  and  $Y^T$  are  $c \times 2$  and  $2 \times t$ , respectively. The pure absorbance–time of  $X(y_X)$ , can be readily measured in the absence of  $L$ , whereas  $y_{XL}$ , is usually unknown. The value  $k'$  can be simply calculated by fitting Eq. 12 the data of the kinetic profile in the absence of  $L$  by a least-squares curve-fitting method using MATLAB. Let

$$R = A - A_Q = A - C_{X,0}y_X^T \quad (20)$$

Here, the concentration profile  $C_{X,0}$  is calculated by optimizing the value of  $K_f$  using Eq. 8. Thus, if  $K_f$  can be resolved, then  $C_{X,0}$  can be optimized. When the rank of  $R$  is one less than the rank of original matrix  $A$ , then the  $C_{X,0}$  is the optimum concentration profile and the obtained  $K_f$  is the optimum formation constant.

$C_{XL,0}$  can then be obtained by Eq. 4. By using RAFA on  $R$ ,  $k''$  can be obtained. By using a suitable  $k''$  value, all of the components of residual matrix become zero (noise level).

$$E = R - A_Q = R - C_{XL,0}y_{XL}^T \quad (21)$$

### Experimental

**Synthetic Data.** To evaluate the performance of the method, a set of kinetic profiles were created. The use of simulated data makes it possible to know how each problem affects the performance of the proposed method.

Parameters setting was as follows:  $k' = 0.07 \text{ s}^{-1}$ ,  $k'' = 0.01 \text{ s}^{-1}$ ,  $C_{X,0} = 5.0 \times 10^{-3} \text{ mol L}^{-1}$ . Measurements were taken from 0 to 300 s with 1 s intervals (301 measuring time in all). The kinetic profiles of all components were produced by a first-order rate equation (Eq. 12 or 18). Vectors of  $X$  and  $XL$  forms were calculated based on Eq. 8, by considering  $K_f = 500 \text{ L mol}^{-1}$  and  $L$  concentrations in the range  $0.001\text{--}0.016 \text{ mol L}^{-1}$  with  $0.003 \text{ mol L}^{-1}$  intervals (6 concentration in all). The kinetic profiles were simulated, and random noise was added to the set of artificial data generated to more rigorously test the method. The error was a set of noise in agreement with the Gaussian distribution with mean zero and standard deviation equal to 0.2% of absorbance value.

**Real Data.** All experiments were performed with analytical reagent grade chemicals purchased from E. Merck. These chemicals were used without further purification. The stock solutions of 4-*tert*-butylcatechol, 3-methylcatechol,  $\beta$ -CD, and  $\text{IO}_3^-$  were prepared by dissolving the compounds in distilled water. Samples were diluted by taking the appropriate aliquots from the stock solutions followed by dilution with phosphate buffer (pH 3.60). The total concentrations of prepared buffers were  $0.15 \text{ mol L}^{-1}$ . Absorption spectra were obtained with a Perkin-Elmer Lambda 45 UV-vis spectrophotometer. In each experiment, the sample placed in a 1 cm path length quartz cells, and the measurements were performed at  $25 \pm 0.1^\circ \text{C}$ .

**Calculations.** All calculations were performed in MATLAB 6.5 (Math Works, Cochituate Place, MA).

### Results and Discussion

**Synthetic Data.** Figure 1a shows created kinetic profiles for the system described above. Based on principal component analysis (PCA), the relative standard deviation (R.S.D.) method is widely used to determine the number of principal compo-

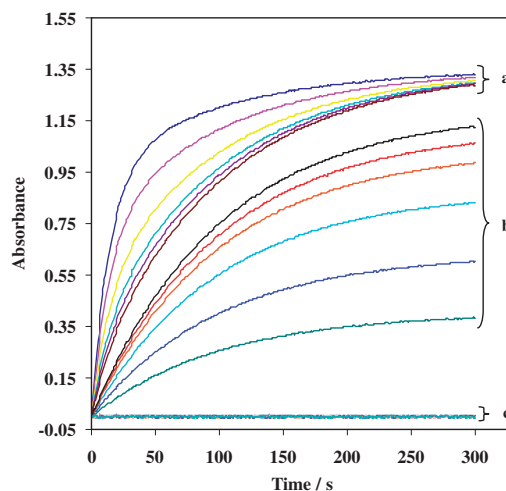


Fig. 1. Simulated absorbance–time plots for a system with  $K_f = 500 \text{ L mol}^{-1}$ ,  $k'' = 0.01 \text{ s}^{-1}$ ,  $k' = 0.07 \text{ s}^{-1}$  at  $C_{X,0} = 5.0 \times 10^{-3} \text{ mol L}^{-1}$  and different  $L$  concentrations (a), after subtraction of  $X$  (b) and after subtraction of  $X$  and  $XL$  kinetic profiles (c) by using RAFA.

Table 1. PCA Results on Simulated Data

$i$	$g_i$	$g_i/g_{i+1}$	R.S.D.
1	46.2076	16.6471	0.0435
2	2.7757	153.0082	0.0068
3	0.0181	1.0541	0.0058
4	0.0172	1.0259	0.0047
5	0.0168		

nents.<sup>24,25</sup>

The R.S.D. is a measure of the lack of fit of a principal component model to a data set. The R.S.D. is defined as<sup>26</sup>

$$\text{R.S.D.}(n) = \left( \frac{\sum_{i=n+1}^c g_i}{(c-n)(t-n)} \right)^{\frac{1}{2}}, \quad (22)$$

where  $g_i$  is the eigenvalue and  $n$  the number of considered principal components. Table 1 presents the eigenvalues, ratios of consecutive eigenvalues, and R.S.D. of matrix  $A$  by PCA. It should be noted that R.S.D. (2) reaches 0.0068, thus satisfying the noise level of the simulative experiment. Also, it should be noted that the ratio of consecutive eigenvalues, when  $n = 2$ , is the maximum at the same time. It also shows that there exist two kinetic profiles in the system, which coincides with the assumption of the simulative experiment.

The value of  $k'$ , for the simulated data in the absence of  $L$  was obtained by least-squares curve fitting of the experimental rate constants using MATLAB. The best  $k'$  is the value that gives the best fit of Eq. 12 through the simulated data.

Simulated data matrix  $A$  was processed by RAFA method. The best estimation of  $K_f$  reduced the rank of the system by one (Fig. 1b). The kinetic profiles in Fig. 1b belonged only to the  $XL$  form. The obtained  $K_f$  was then used to estimate of  $k''$ . The best estimation of  $k''$  reduced the rank of the system to zero (noise level) (Fig. 1c). The relationship between R.S.D. of matrices  $R$  and  $E$  and the estimaties for  $K_f$  and  $k''$  are shown

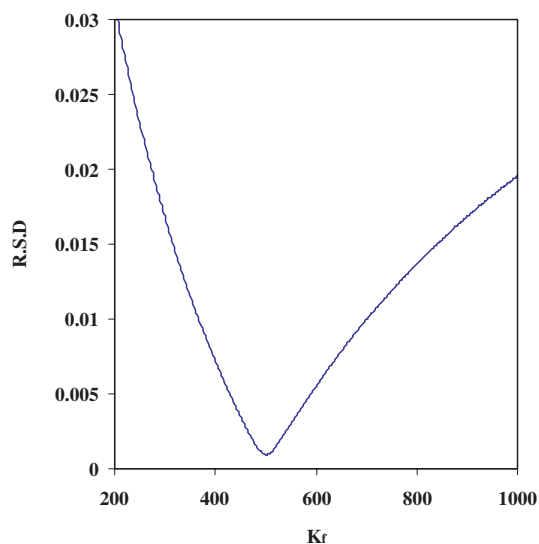


Fig. 2. Relationship between R.S.D. and  $K_f$  for simulated data.

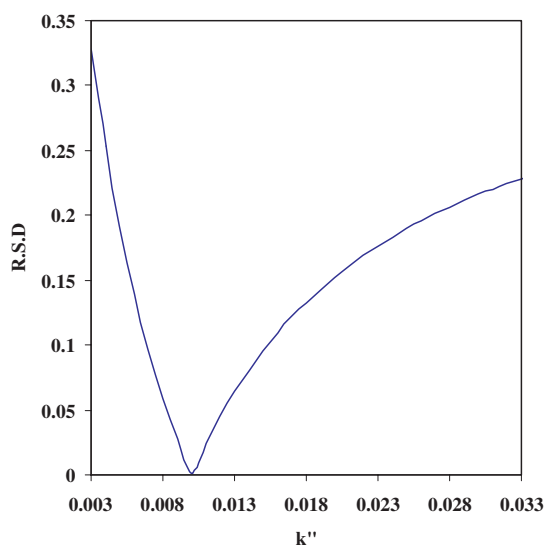
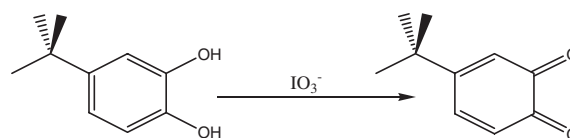


Fig. 3. Relationship between R.S.D. and  $k''$  for simulated data.

as R.S.D. curve in Figs. 2 and 3, respectively. For each value of  $K_f$  and  $k''$ ,  $C_{X,0}$  and  $y_{XL}$  were calculated, and matrices  $R$  and  $E$  were obtained. Narrow minimums were observed in the R.S.D. curves shown in Figs. 2 and 3, which indicate the optimum estimations of  $K_f$  and  $k''$ .

**Experimental Data.** The spectrophotometric data obtained from the investigation of the effect of  $\beta$ -CD concentration on the oxidation reaction of 4-*tert*-butylcatechol and 3-methylcatechol with iodate at pH 3.60 was used as experimental data. The chemical or electrochemical oxidation of catechol derivatives and catecholamines has previously been studied.<sup>27</sup> These compounds form 1:1 inclusion complexes with  $\beta$ -CD.<sup>23</sup> It was observed that the absorption spectrum for the inclusion complex were the same as those for the catechol derivatives. Catechol derivatives can be oxidized chemically to their corresponding *o*-quinones by using the proper oxidants, such as iodate (Scheme 1).

Iodate oxidizes catechol derivatives to their corresponding



Scheme 1.

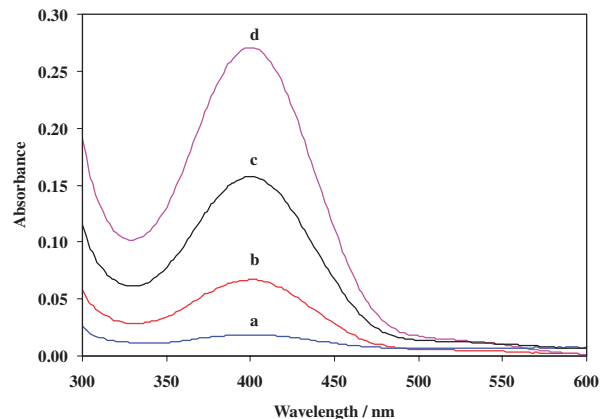


Fig. 4. Absorption spectra for  $2.0 \times 10^{-4} \text{ mol L}^{-1}$  4-*tert*-butylcatechol with time in the presence of  $0.01 \text{ mol L}^{-1}$   $\text{IO}_3^-$  at pH 3.60. In the presence of  $5.0 \times 10^{-3} \text{ mol L}^{-1}$  of  $\beta$ -CD (a, c) and in the absence of  $\beta$ -CD (b, d) at 40 s (a, b) and 520 s (c, d).

*o*-quinones. The rate of the reaction is very fast at low pH values and decreases with an increase in the pH of the solution. We observed that at pH 3.60, the rate of the reaction was not very fast and the reaction could be monitored spectrophotometrically.

Figure 4 shows the absorption spectra for 4-*tert*-butylcatechol versus time in the presence of iodate at pH 3.60. The absorbance of the solution increased with time at 400 nm, which shows that 4-*tert*-butylcatechol is oxidized to its corresponding *o*-quinone. In order to monitor the oxidation reaction of 4-*tert*-butylcatechol with iodate, the absorbance changes at 400 nm were monitored. The kinetic profiles for the oxidation reaction of  $2.0 \times 10^{-4} \text{ mol L}^{-1}$  4-*tert*-butylcatechol with  $0.01 \text{ mol L}^{-1}$  iodate at pH 3.60 in the presence of different concentrations of  $\beta$ -CD at 400 nm are shown in Fig. 5.

The pseudo-first-order rate constant for the oxidation reaction of 4-*tert*-butylcatechol in the absence of  $\beta$ -CD, i.e.,  $k'$ , was determined to be  $0.0066 \text{ s}^{-1}$  by least-squares curve fitting of the experimental data on Eq. 12 using MATLAB. The best estimation for  $k'$  is the value for which R.S.D. is a minimum.

As Figure 5 shows, the reaction rate decreased with an increase in the  $\beta$ -CD concentration. Addition of  $\beta$ -CD to the 4-*tert*-butylcatechol causes formation of a 1:1 inclusion complex between them.<sup>23</sup> The decrease in the rate of the reaction by addition of  $\beta$ -CD indicates that the rate constant for the oxidation of complexed form of 4-*tert*-butylcatechol is smaller than that of its free form. The rate constants for the electron-transfer reactions decreased substantially upon inclusion of the reductant, due to steric hindrance, which affects donor-acceptor orbital overlap. Therefore, the change in the reaction rate as a function of  $\beta$ -CD concentration could be used to determine the stability constant of the produced inclusion complex.

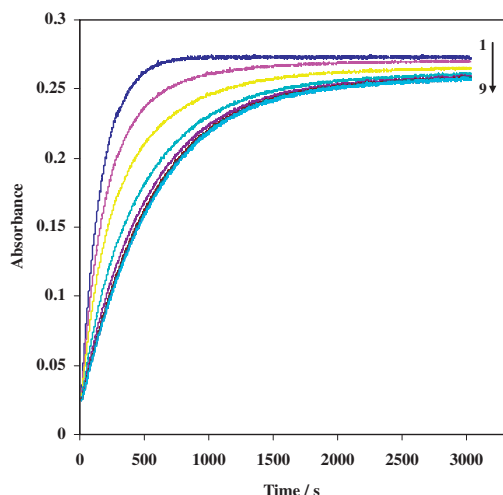


Fig. 5. The absorbance–time plots for the oxidation reaction of  $2.0 \times 10^{-4} \text{ mol L}^{-1}$  4-*tert*-butylcatechol with  $0.01 \text{ mol L}^{-1} \text{ IO}_3^-$  at pH 3.60 in the presence of (1) 0.0, (2)  $1.0 \times 10^{-4}$ , (3)  $2.0 \times 10^{-4}$ , (4)  $5.0 \times 10^{-4}$ , (5)  $1.0 \times 10^{-3}$ , (6)  $2.0 \times 10^{-3}$ , (7)  $3.0 \times 10^{-3}$ , (8)  $4.0 \times 10^{-3}$ , and (9)  $5.0 \times 10^{-3} \text{ mol L}^{-1}$  of  $\beta$ -CD at 400 nm.

Table 2. Results of PCA on Experimental Data for 4-*tert*-Butylcatechol ( $2.0 \times 10^{-4} \text{ mol L}^{-1}$ ) in the Presence of  $0.01 \text{ mol L}^{-1} \text{ IO}_3^-$  and Different Concentrations of  $\beta$ -CD

$i$	$g_i$	$g_i/g_{i+1}$	R.S.D.
1	38.5211	21.1375	0.0095
2	1.8224	114.6164	0.0017
3	0.0159	1.7472	0.0015
4	0.0091	1.0706	0.0013
5	0.0085		

The kinetic profiles, where were determined by applying PCA on data matrix, are shown in Fig. 5. The results are presented in Table 2. The ratio of consecutive eigenvalues reached a maximum at  $n = 2$ , which indicates that there are two kinetic profiles in the experimental absorbance–time system.  $K_f$  and  $k''$  were optimized by the proposed method and the relationships between R.S.D. and  $K_f$  and R.S.D. and  $k''$  are shown in Figs. 6 and 7, respectively. The optimal set solutions were  $K_f = 8890 \text{ L mol}^{-1}$  with R.S.D = 0.0010 and  $k'' = 0.0016 \text{ s}^{-1}$  with R.S.D = 0.0011. The above experiments were repeated with different excess concentrations of iodate under pseudo-first-order reaction conditions. The results are given in Table 3. Figure 8 shows the plots of  $k'$  and  $k''$  as a function of iodate concentration. As it was expected,  $k'$  and  $k''$  increased linearly with an increase in the iodate concentration. Since  $k' = k_1 [\text{IO}_3^-]$  and  $k'' = k_2 [\text{IO}_3^-]$ , where  $k_1$  and  $k_2$  are the rate constants for free and complexed catechol derivatives, respectively, therefore the value of  $k_1$  and  $k_2$  can be obtained from the slopes of the plots, and  $k_1$  and  $k_2$  were 0.595 and  $0.152 \text{ L mol}^{-1} \text{ s}^{-1}$ , respectively.

The oxidation reaction of 3-methylcatechol in the presence of  $\beta$ -CD was also investigated at pH 3.60 by the same methods as described for 4-*tert*-butylcatechol. Figure 9a shows the absorbance–time plots for the oxidation reactions of  $5.0 \times$

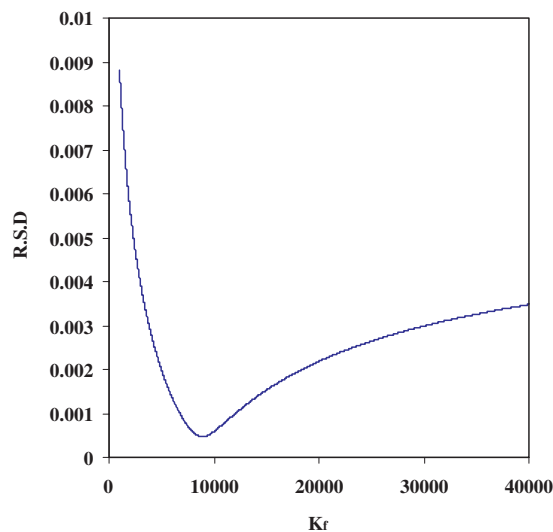


Fig. 6. Relationship between R.S.D. and  $K_f$  for  $2.0 \times 10^{-4} \text{ mol L}^{-1}$  4-*tert*-butylcatechol in the presence of  $0.01 \text{ mol L}^{-1} \text{ IO}_3^-$  and different concentrations of  $\beta$ -CD.

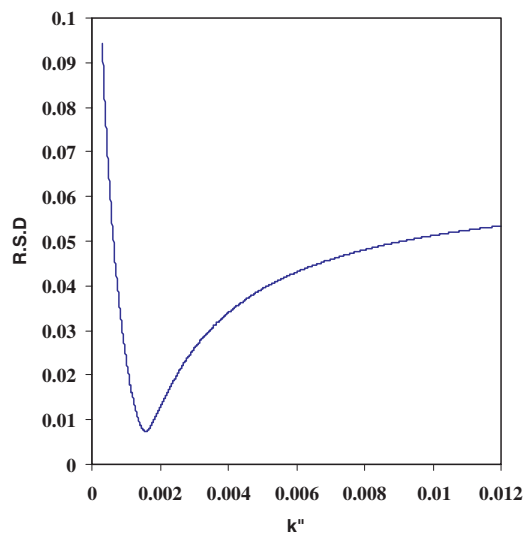


Fig. 7. Relationship between R.S.D. and  $k''$  estimations for  $2.0 \times 10^{-4} \text{ mol L}^{-1}$  4-*tert*-butylcatechol in the presence of  $0.01 \text{ mol L}^{-1} \text{ IO}_3^-$  and different concentrations of  $\beta$ -CD.

Table 3.  $K_f$  for the Inclusion Complexes of 4-*tert*-Butylcatechol ( $2.0 \times 10^{-4} \text{ mol L}^{-1}$ ) and  $\beta$ -CD and  $k'$  and  $k''$  for the Oxidation of Its Free and Complexed Forms with Different Concentrations of Iodate at pH 3.60

$\text{IO}_3^-/\text{mol L}^{-1}$	$K_f/\text{L mol}^{-1}$	$k'/\text{s}^{-1}$	$k''/\text{s}^{-1}$
0.005	9168	0.0026	0.00085
0.007	9861	0.0043	0.00130
0.010	8890	0.0066	0.00160
0.014	9032	0.0081	0.0020
0.018	9620	0.0110	0.0030

$10^{-4} \text{ mol L}^{-1}$  3-methylcatechol in the presence of different concentrations of  $\beta$ -CD with  $0.021 \text{ mol L}^{-1}$  iodate at pH 3.60. The experimental data matrix of 3-methylcatechol

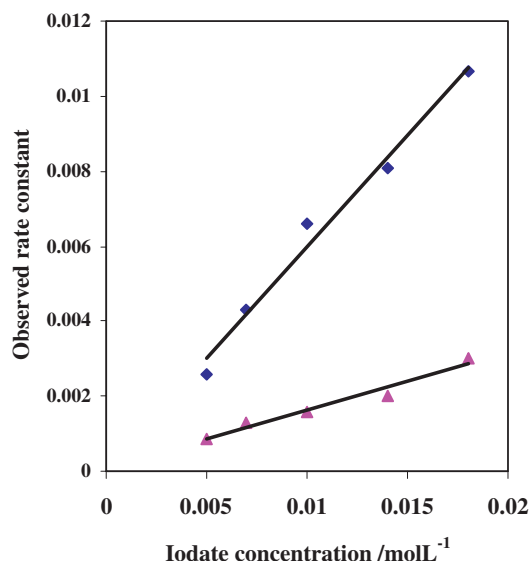


Fig. 8.  $k'$  (■) and  $k''$  (▲) for the oxidation of 4-*tert*-butylcatechol as a function of  $\text{IO}_3^-$  concentration at pH 3.60.

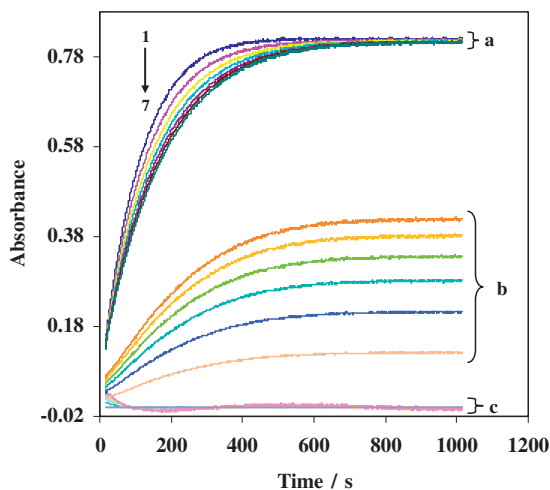


Fig. 9. The absorbance–time plots for the oxidation of a  $5.0 \times 10^{-4} \text{ mol L}^{-1}$  3-methylcatechol with  $0.021 \text{ mol L}^{-1}$   $\text{IO}_3^-$  at pH 3.60 in the presence of (1) 0.0, (2)  $3.0 \times 10^{-3}$ , (3)  $6.0 \times 10^{-3}$ , (4)  $9.0 \times 10^{-3}$ , (5)  $1.2 \times 10^{-2}$ , (6)  $1.5 \times 10^{-2}$ , and (7)  $1.8 \times 10^{-2} \text{ mol L}^{-1}$  of  $\beta\text{-CD}$  (a) after substituting the free form, (b) after substituting the free and the complex kinetic profiles and (c) by using RAFA.

was investigated with PCA and the eigenvalues and the ratios of consecutive eigenvalues shows two kinetic profiles in absorbance–time plots (Table 4).

The  $k'$  values were obtained by using the same method as described for 4-*tert*-butylcatechol. The RAFA method was used for analysis of the mentioned system, and the  $K_f$  and  $k''$  estimations for 3-methylcatechol in the presence of different concentrations of  $\beta\text{-CD}$  and  $0.021 \text{ mol L}^{-1}$  of  $\text{IO}_3^-$  were obtained. The estimations are  $K_f = 61 \text{ L mol}^{-1}$  with R.S.D = 0.002 and  $k'' = 0.0047 \text{ s}^{-1}$  with R.S.D = 0.0044.

Figure 9b shows the absorbance–time plots with the kinetic profiles of the free form subtracted. After substituting of the kinetic profiles of the free and the complex forms from the data

Table 4. Results of PCA on Experimental Data for 3-Methylcatechol ( $5.0 \times 10^{-4} \text{ mol L}^{-1}$ ) in the Presence of  $0.021 \text{ mol L}^{-1}$   $\text{IO}_3^-$  at Different Concentrations of  $\beta\text{-CD}$  at pH 3.60

$i$	$g_i$	$g_i/g_{i+1}$	R.S.D.
1	61.8094	47.8607	0.0149
2	1.2914	136.6143	0.0027
3	0.0095	1.0325	0.0024
4	0.0092	1.0092	0.0020
5	0.0091		

Table 5.  $K_f$  for the Inclusion Complexes of 3-Methylcatechol ( $5.0 \times 10^{-4} \text{ mol L}^{-1}$ ) and  $\beta\text{-CD}$ , and  $k'$  and  $k''$  for the Oxidation of Its Free and Complexed Forms with Different Concentrations of Iodate at pH 3.60

$\text{IO}_3^-/\text{mol L}^{-1}$	$K_f/\text{L mol}^{-1}$	$k'/\text{s}^{-1}$	$k''/\text{s}^{-1}$
0.0060	57	0.0036	0.0017
0.0016	58	0.0085	0.0040
0.0210	61	0.0101	0.0047
0.0300	62	0.0137	0.0057

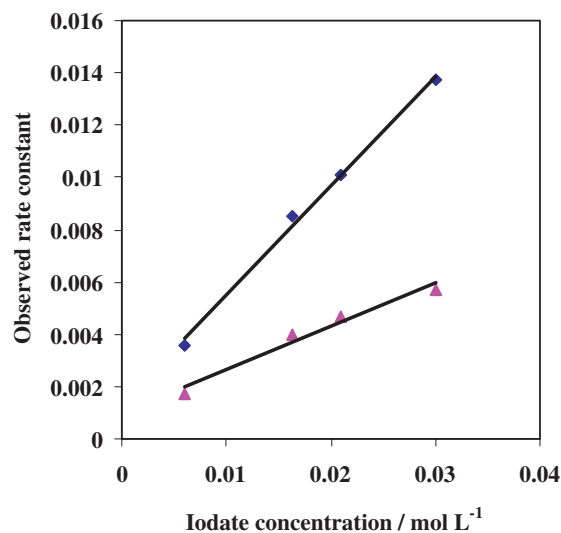


Fig. 10.  $k'$  (■) and  $k''$  (▲) for the oxidation of 3-methylcatechol as a function of iodate concentration at pH 3.60.

matrix based on the optimum  $K_f$  and  $k''$  estimations, the components of residual matrix reached to noise level (Fig. 9c).

The values of  $K_f$ ,  $k'$ , and  $k''$  were estimated for 3-methylcatechol in the absence and presence of different concentrations of  $\beta\text{-CD}$  and at various concentrations of  $\text{IO}_3^-$  by using the same method as described for 4-*tert*-butylcatechol. The values are reported in Table 5. As for 4-*tert*-butylcatechol,  $k'$  and  $k''$  increased linearly with an increase in the  $\text{IO}_3^-$  concentrations (Fig. 10). The values  $k_1$  and  $k_2$  ( $\text{L mol}^{-1} \text{ s}^{-1}$ ) were determined from the slope of the best fit line on this curve to be 0.418 and  $0.167 \text{ L mol}^{-1} \text{ s}^{-1}$ , respectively.

### Conclusion

The proposed method is simple, very sensitive and easy to understand and apply. It was suitable for the spectrophotometric determination of the stability constants of the nonabsorbing

complexes or complexes that have the same absorption spectra as those for the reactants. The method could be used to determine the stability constant of complex XL when X (or L) reacts with a suitable reagent, e.g., Z. The kinetic profiles at different concentrations of L (or X) could be obtained to create a two-way data matrix. The kinetic profiles were obtained by monitoring the change in the absorbance of the products or X (or L) or Z at the proper wavelength with time. The rate constants for both the reactions of X and XL with Z were obtained. RAFA is an efficient chemometrics algorithm for complete analysis of kinetic profiles. It should be noted that for obtaining the kinetic profiles by measuring the absorbance of products at a single wavelength, the absorption spectra of the products of the reaction X (or L) and XL with Z should be the same or overlap with each other.

Comparison of  $K_f$  for the investigated catechol derivatives indicates that the complex of  $\beta$ -CD with 4-*tert*-butylcatechol is more stable than that with 3-methylcatechol. This is not unexpected because for strong inclusion, the guest molecule must fit tightly with the CD cavity and be hydrophobic in nature.<sup>28</sup> The amount of  $K_f$  for 4-*tert*-butylcatechol obtained by the proposed method ( $(9.31 \pm 0.4) \times 10^3 \text{ L mol}^{-1}$ ) was in good agreement with the previously reported value ( $(9.50 \pm 2.0) \times 10^3 \text{ L mol}^{-1}$ ).<sup>23</sup> Thus, the proposed method can be applied to the any complexation or association systems with strong or weak interactions.

#### References

- 1 R. X. Cai, X. G. Wu, Z. H. Liu, W. H. Ma, *Analyst* **1999**, *124*, 751.
- 2 R. X. Cai, X. G. Wu, Z. X. Lin, J. K. Chen, *Chem. J. Chin. Univ.* **1997**, *18*, 364.
- 3 S. Bijlsma, D. J. Louwerse, W. Windig, A. K. Smilde, *Anal. Chim. Acta* **1998**, *376*, 339.
- 4 S. Bijlsma, D. J. Louwerse, A. K. Smilde, *J. Chemom.* **1999**, *13*, 311.
- 5 E. Furusjö, L. G. Danielsson, *Anal. Chim. Acta* **1998**, *373*, 83.
- 6 Y. Z. Liang, *White, Gray and Black Multicomponent Systems and Their Chemometric Algorithms*, Hunan Publishing House of Science and Technology, Changsha, **1996**, pp. 102–107.
- 7 C. N. Ho, G. D. Christian, E. R. Davidson, *Anal. Chem.* **1978**, *50*, 1108.
- 8 A. Lorber, *Anal. Chim. Acta* **1984**, *164*, 293.
- 9 A. Lorber, *Anal. Chem.* **1985**, *57*, 2395.
- 10 E. Sanchez, B. R. Kowalski, *Anal. Chem.* **1986**, *58*, 496.
- 11 D. H. Burns, J. B. Callis, G. D. Christian, *Anal. Chem.* **1986**, *58*, 2805.
- 12 T. Roch, *Anal. Chim. Acta* **1997**, *356*, 61.
- 13 J. L. Beltrán, R. Ferrer, J. Guiteras, *Anal. Chim. Acta* **1998**, *373*, 311.
- 14 M. Maeder, Y.-M. Neuhold, A. Olsen, G. Puxty, R. Dyson, A. Zilian, *Anal. Chim. Acta* **2002**, *464*, 249.
- 15 H. Abdollahi, F. Nazari, *Anal. Chim. Acta* **2003**, *486*, 109.
- 16 A. Afkhami, L. Khalafi, *Anal. Chim. Acta* **2006**, *569*, 267.
- 17 Z.-L. Zhu, J. Xia, J. Zhang, T.-H. Li, *Anal. Chim. Acta* **2002**, *454*, 21.
- 18 Z.-L. Zhu, W. Li, J. Xia, *Anal. Chim.* **2004**, *527*, 203.
- 19 M. L. Bender, M. Komiyama, *Cyclodextrin Chemistry*, Springer Verlag Berlin, **1978**.
- 20 K. A. Connors, *Chem. Rev.* **1997**, *97*, 1325.
- 21 M. V. Rekharsky, Y. Inoue, *Chem. Rev.* **1998**, *98*, 1875.
- 22 H.-J. Schneider, *Angew. Chem., Int. Ed. Engl.* **1991**, *30*, 1417.
- 23 J. A. Imonigie, D. H. Macartney, *Inorg. Chem.* **1993**, *32*, 1007.
- 24 E. R. Malinowski, *Factor Analysis in Chemistry*, 2nd ed., Wiley, New York, **1991**.
- 25 A. Elbergali, J. Nygren, M. Kubista, *Anal. Chim. Acta* **1999**, *379*, 143.
- 26 N. M. Faber, L. M. C. Buydens, G. Kateman, *Chemom. Intell. Lab. Syst.* **1994**, *25*, 203.
- 27 A. Afkhami, D. Nematollahi, L. Khalafi, M. Rafiee, *Int. J. Chem. Kinet.* **2005**, *37*, 17.
- 28 M. D. Johnson, V. C. Reinsborough, S. Ward, *Inorg. Chem.* **1992**, *31*, 1085.